$^{40}Ar/^{39}Ar$ dating of volcanism and subsequent very low-grade metamorphism in a subsiding basin: example of the Cretaceous lava series from central Chile

Francisco Fuentes[a], Gilbert Féraud[b,*], Luis Aguirre[a], Diego Morata[a]

[a]*Departamento de Geología, Universidad de Chile, Casilla 13518, Correo 21, Santiago, Chile*
[b]*UMR 6526 Géosciences Azur, CNRS-UNSA, Université de Nice-Sophia Antipolis, 06108 Nice Cedex 02, France*

Abstract

$^{40}Ar/^{39}Ar$ geochronological method is applied to date both emplacement and subsequent very low-grade metamorphism of a thick lava series, the Veta Negra Formation from the Cordón de Chacana area, in the Coastal Range of central Chile. On the same lava series, and even on the same rock sample, it was possible to measure apparently valid ages of both the emplacement of lava flows (by dating transparent plagioclase) and the very low-grade metamorphic event (by dating sericite and/or adularia). Sericite was dated on step heated single grains of strongly altered plagioclases, the radiogenic argon from remaining fresh plagioclase appearing as negligible on most part of the age spectrum. The concordance between one plateau age of 118.7 ± 0.6 Ma displayed by fresh plagioclase and a previously measured plateau age on plagioclase from one lava flow from a region due west from Santiago [Bustamante Hill, Aguirre, L., Féraud, G., Morata, D., Vergara, M., Robinson, D., 1999. Time interval between volcanism and burial metamorphism and rate of basin subsidence in a Cretaceous Andean extensional setting. Tectonophysics 313, 433–447] may indicate that the volcanic activity of the Veta Negra Formation was synchronous along the 80-km long latitudinal segment studied. Ages of 96.8 ± 0.2 and 97.0 ± 1.6 Ma displayed by adularia and sericite (respectively) are slightly older than ages of 93–94 Ma given by adularia from the Bustamante Hill. These data allow to define a period of about 22 Ma between volcanism and metamorphism. Because of the contemporaneity of some metamorphic minerals and Cretaceous plutons of the region, the very low-grade metamorphic event may be the result of the additional effect of burial and a regional thermal event. Nevertheless, a significant effect of burial (relatively to the contribution of high thermal gradient event(s)) seems revealed by an apparent age gradient on very low-grade minerals with the stratigraphic depth.

Keywords: Very low-grade metamorphism; Dating; $^{40}Ar/^{39}Ar$; Chile; Cretaceous; Plagioclase

1. Introduction

The time interval between deposition of volcanic materials in a regionally subsiding basin and the

* Corresponding author. Fax: +33 492 0768 16.
E-mail addresses: ffuentes@cec.uchile.cl (F. Fuentes), feraud@unice.fr (G. Féraud), luaguirr@cec.uchile.cl (L. Aguirre), dmorata@cec.uchile.cl (D. Morata).

generation of very low-grade metamorphic assemblages in those same materials due to burial and/or subsequent thermal event is a scarcely quantified subject (see Åberg et al., 1984; Åberg, 1985; Aguirre et al., 1999). This situation is mainly due to the reduced number of mineral phases compositionally suitable to apply methods such as the $^{40}Ar/^{39}Ar$ on the one hand and, on the other, because of the small amount in which these phases are commonly found. Among them, the K-feldspar adularia, the sericitic micas and the celadonites are the best known examples of K-bearing secondary minerals present in metabasites in sub-greenschist facies. Moreover, when secondary mineral phases are well developed,

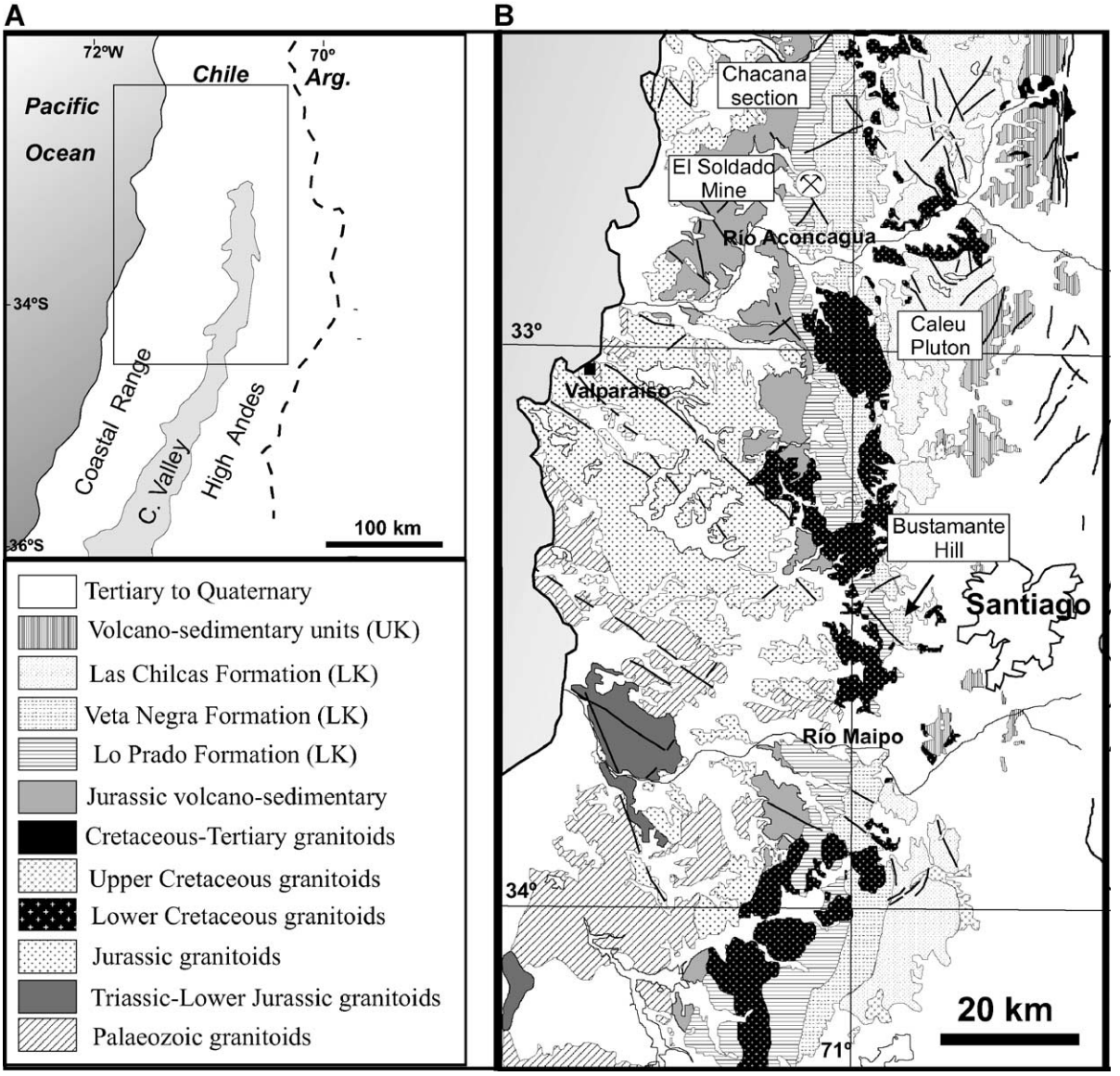

Fig. 1. (A) Main physiographic features of central Chile. Arg.=Argentina, C. Valley=Central Valley Graben. (B) Geological sketch map of the Coastal Range between 32°30′S and 34°S showing the studied areas and the strata-bound El Soldado copper deposit. LK=Lower Cretaceous; UJ, MJ and LJ=Upper, Medium and Lower Jurassic, respectively (simplified from the 1/1,000,000 geological map of Chile, Sernageomin, 2002).

primary minerals are generally too altered to allow correct dating of volcanism.

Recently, geochronological research directed to quantify the interval volcanism-metamorphism by the $^{40}Ar/^{39}Ar$ method has been successfully conducted in the Coastal Range of central Chile due west from Santiago, at the Bustamante Hill area (Fig. 1), where Early Cretaceous volcanism is typically represented. A value of ca. 25 Ma was obtained for the interval in this area (Aguirre et al., 1999). This research has been later extended to the area of Cordón de Chacana (Fig. 1), about 80 km further north, where the same early Cretaceous volcanic sequences are exposed. New geochronological data obtained there confirm the previous age of the volcanism,. Moreover, we could also successfully test a new methodological approach to the age determination of the metamorphic events in these type of rocks, which consists in dating co-existing adularia and sericite (analyzed in altered single grains of plagioclase) as part of the same mineral parageneses.

2. Geological framework

A 3–13-km-thick and ca. 1200-km long volcanic belt of early Cretaceous age is exposed along the Coastal Range of central Chile (Fig. 1). Between latitudes 33°25′S (Bustamante Hill) and 32°35′S (Cordón de Chacana), the belt is mainly represented by the Veta Negra Formation, a thick pile of continental porphyritic basalts and basaltic andesites, 3.5–5.0 km thick, with high-K calc-alkaline and shoshonitic affinities (Levi et al., 1988; Vergara et al., 1995). The flows in this formation have distinct porphyritic texture characterized by abundant and large (up to 2 cm) plagioclase ($An_{56}Ab_{40}Or_4$ to $An_{70}Ab_{28}Or_2$) phenocrysts, subordinate augite ($Wo_{38}En_{45}Fs_{17}$), titanomagnetite and small amounts of totally altered olivine crystals. The flows of the Veta Negra Formation were deposited in an extensional ensialic setting corresponding to a subsiding intra-arc or back-arc basin (Åberg et al., 1984; Vergara et al., 1995).

The rocks of the Veta Negra Formation have been affected by very low-grade non-deformative metamorphism, which preserved the primary structures and textures. This metamorphism, in the prehnite-pumpellyite facies, is characterized by a grade, which regularly increases with the stratigraphic depth. Regional facies boundaries are parallel or subparallel to bedding and not to contact with contemporaneous or younger granitoids in the area demonstrating that this metamorphism is unrelated directly to the intrusions. These characteristics conform to the classical definition of burial metamorphism (Coombs, 1960) and correspond to the diastathermal (extensional) metamorphism as described by Robinson (1987). Nevertheless, we shall see that the age of this metamorphism being contemporaneous with at least one of these intrusions (Caleu pluton: Fig. 1), very low-grade metamorphism is also probably partly influenced by a regional thermal event.

The metamorphic minerals are found in different metadomains among which: (i) partially or totally replaced primary minerals, (ii) altered glassy material from the groundmass, (iii) amygdale infilling and (iv) veinlets and microfractures. Metamorphic feldspars appear: (1) replacing primary phenocrysts and microliths of plagioclase and (2) filling open spaces, e.g., amygdales and veinlets. In (1), they correspond to pure albite resulting from albitization processes and to K-feldspar (adularia) as patches inside totally albitized plagioclase phenocrysts; sericite flakes accompany these feldspars. In (2), adularia ($Or_{97}Ab_3$) is abundantly present filling amygdales in low-variance assemblages together with pumpellyite, chlorite, low albite and scarce sericite (Morata et al., 1997).

3. Sampling and analytical procedures

The 2-km-thick section of the Veta Negra Formation from the Cordón de Chacana was studied in detail and four samples (CHAC8, CHAC18, CHAC19, CHAC22) were selected for dating (Fig. 2). They are located at the lower-central part of the Lower Cretaceous series. Analyzed transparent and strongly sericitized plagioclase crystals belong to the same lava flow. Analyzed adularia crystals were selected from amygdales from the top of the same lava flow and from a contiguous flow.

Crystals of: (i) transparent plagioclase, (ii) strongly sericitized plagioclase and (iii) adularia were analysed by the $^{40}Ar/^{39}Ar$ step heating procedure. Plagioclase (CHAC8, CHAC19: 160–200 μm fraction) were separated from two samples of the basic flows from

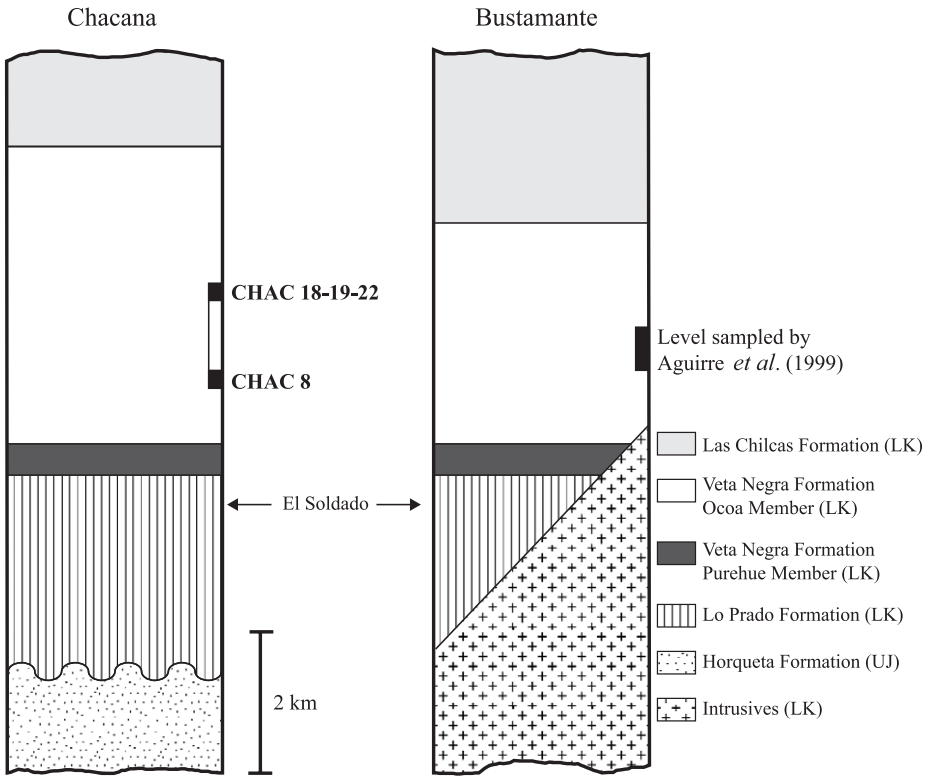

Fig. 2. Position of the analyzed samples in stratigraphic columns of the early Cretaceous for the Cordón de Chacana (this study) and the Bustamante Hill (Aguirre et al., 1999). The approximate location of the strata-bound El Soldado copper deposit is indicated. LK=Lower Cretaceous, UJ=Upper Jurassic.

the Veta Negra Formation using a magnetic separator, then carefully selected under a binocular microscope in order to analyse a ca. 20-mg fraction or small clusters (30–32) of transparent grains only. The most milky-white plagioclase crystals (strongly sericitized), 500–1000 μm in size, were also selected in order to analyse sericite directly in plagioclase (discrete sericite crystals cannot be separated from plagioclase) Crystals of adularia between 800 and 1500 μm in size, were directly hand-picked from amygdales in two lava samples (CHAC18, CHAC22) from the Veta Negra Formation, and then carefully selected under the binocular microscope.

All the samples were irradiated in position 5 c for 25 or 75 h in the nuclear reactor of the McMaster University, Hamilton, Canada. The total neutron flux density during irradiation was 3.15 and 8.8×10^{18} N cm^{-2} (two distinct irradiations), with a maximum flux gradient estimated at $\pm0.2\%$ in the volume containing the samples. Argon analyses were performed in Nice (France). The Fish Canyon sanidine (FCs), with an age of 28.02 Ma (Renne et al., 1998), was used as a flux monitor. The plagioclase bulk samples were step heated with a high frequency furnace, connected to a 120°/12 cm MASSE mass spectrometer working with a Baür-Signer GS 98 source and a Balzers SEV 217 electron multiplier. For single grains of adularia, and sericitized plagioclase, and small clusters of transparent plagioclase grains, gas extraction was carried out with a CO_2 Synrad 48-5 continuous laser; the mass spectrometer is a VG 3600 working with a Daly detector system. The typical blank values for the extraction and purification laser system, which are currently measured every third step, were in the range $1.4–10\times10^{-13}$ ccSTP for ^{40}Ar, $0.4–4.5\times10^{-14}$ ccSTP for ^{39}Ar, $0.7–1.4\times10^{-13}$ ccSTP for ^{37}Ar and $2–3\times10^{-14}$ ccSTP for ^{36}Ar. The criteria for defining plateau ages were the following: (1) it should contain at least 70% of released ^{39}Ar, (2) there should be at least three successive steps in the plateau and (3) the

integrated age of the plateau should agree with each apparent age of the plateau within a 2σ error confidence interval. Uncertainties on the apparent ages on each step are quoted at the 1σ level and do not include the errors on the $^{40}Ar^*/^{39}Ar_K$ ratio and the age of the monitor. Errors on plateau and isochron ages are given at the 2σ level. The error on the $^{40}Ar^*/^{39}Ar_K$ ratio of the monitor is included in the plateau age error bar calculation.

X-ray diffraction analyses were performed at the Servicio Nacional de Geología y Minería (SERNAGEOMIN), Chile, with a Philips 1130-90 diffractometer, CuKα radiation, 40 kV, 20 nA, Ni filter and divergence slit of 1°. Chemical composition of primary and secondary minerals were obtained using a CAMECA SX-50 electron microprobe (20 kV, 20 nA and 3 μ as analytical conditions) at the Centro de Instrumentación Científica of the University of Granada (Spain) and a CAMECA SU-30 SEM-probe (15 kV, 10 nA, 3–5 μ as analytical conditions) at the Departamento de Geología, University of Chile (Chile). Back-scattered images were also performed in the CAMECA SU-30 SEM-probe.

4. Mineral chemistry and crystal structure

Chemical compositions of plagioclase, adularia and sericite contained in plagioclase crystals were obtained by microprobe analyses and are shown in Table 1. Almost unzoned primary plagioclase compositions range from $An_{51}Ab_{46}Or_3$ to $An_{61}Ab_{36}Or_3$. The two crystals of adularia analysed come from amygdales where they are in contact with pumpellyite, chlorite/smectite, albite and scarce sericite (CHAC18, Fig. 3a) or with chlorite/smectite (CHAC22, Fig. 3c). Their compositions are close to pure K-feldspar ($An_{2-0}Ab_{2-1}Or_{96-99}$ in CHAC18 and $Ab_{4-2}Or_{96-98}$ in CHAC19). Pure sericites (Table 1) are only present as small crystals in plagioclases (Fig. 3d).

Table 1
Selected microprobe analyses of feldspars from the Chacana section of lava flows (central Chile)

Sample	CHAC8	CHAC8	CHAC19	CHAC19	CHAC18	CHAC19	CHAC18	CHAC22	CHAC8	CHAC19
Analysis	69	70	88	89	71	80	43	25	72	86
Notes	Pl, p, c	Pl, p, r	Pl, p, c	Pl, p, r	AbPl, p	AbPl, p	Ad, a	Ad, a	SrdPl, p	SrdPl, p
SiO_2	54.66	54.30	55.68	56.19	69.27	70.73	66.32	63.88	55.55	54.45
TiO_2	0.07	0.00	0.17	0.10	0.00	0.05	0.10	0.01	0.00	0.05
Al_2O_3	28.45	28.27	27.96	27.15	21.22	21.30	17.89	18.64	30.04	33.17
FeO	0.78	0.90	1.03	1.01	0.13	0.08	0.00	0.05	0.81	1.28
MnO	0.00	0.00	0.00	0.01	0.17	0.00	0.00	0.00	0.00	0.26
MgO	0.07	0.07	0.13	0.07	0.00	0.00	0.00	0.01	0.20	0.32
CaO	12.11	11.53	11.47	10.83	0.96	2.03	0.29	0.00	0.91	0.29
Na_2O	4.58	4.81	5.08	5.16	6.68	6.62	0.21	0.20	2.42	0.72
K_2O	0.54	0.53	0.46	0.47	0.63	0.11	14.46	16.23	6.46	8.16
Sum	101.26	100.42	101.99	100.98	99.06	100.92	99.26	99.02	96.40	98.68
N. Ox	*8*	*8*	*8*	*8*	*8*	*8*	*8*	*8*	*22*	*22*
Si	2.543	2.457	2.480	2.520	3.008	3.011	3.047	2.983	7.079	6.822
Ti	0.002	0.000	0.006	0.003	0.000	0.002	0.003	0.000	0.000	0.005
Al	1.505	1.508	1.468	1.435	1.086	1.068	0.968	1.026	4.512	4.899
Fe	0.029	0.034	0.038	0.038	0.005	0.003	0.000	0.002	0.087	0.134
Mn	0.000	0.000	0.000	0.000	0.006	0.000	0.000	0.000	0.000	0.028
Mg	0.005	0.005	0.009	0.005	0.000	0.000	0.000	0.001	0.038	0.059
Ca	0.582	0.559	0.548	0.520	0.044	0.093	0.014	0.000	0.124	0.038
Na	0.398	0.422	0.438	0.449	0.563	0.546	0.018	0.019	0.599	0.175
K	0.031	0.031	0.026	0.027	0.035	0.006	0.847	0.967	1.050	1.304
Σcations	5.006	5.015	5.013	4.997	4.747	4.729	4.899	4.997	13.489	13.464
%An	57.56	55.26	54.09	52.26	6.92	14.34	1.61	0.02		
%Ab	39.37	41.70	43.31	45.05	87.63	84.71	2.08	1.88		
%Or	3.06	3.04	2.60	2.69	5.45	0.95	96.32	98.10		

Pl=fresh plagioclase, AbPl=albitized plaglioclase, Ad=adularia, SrdPl=sericitized plagioclasa, p=phenocrysts, c=core, r=rim, a=amygdales.

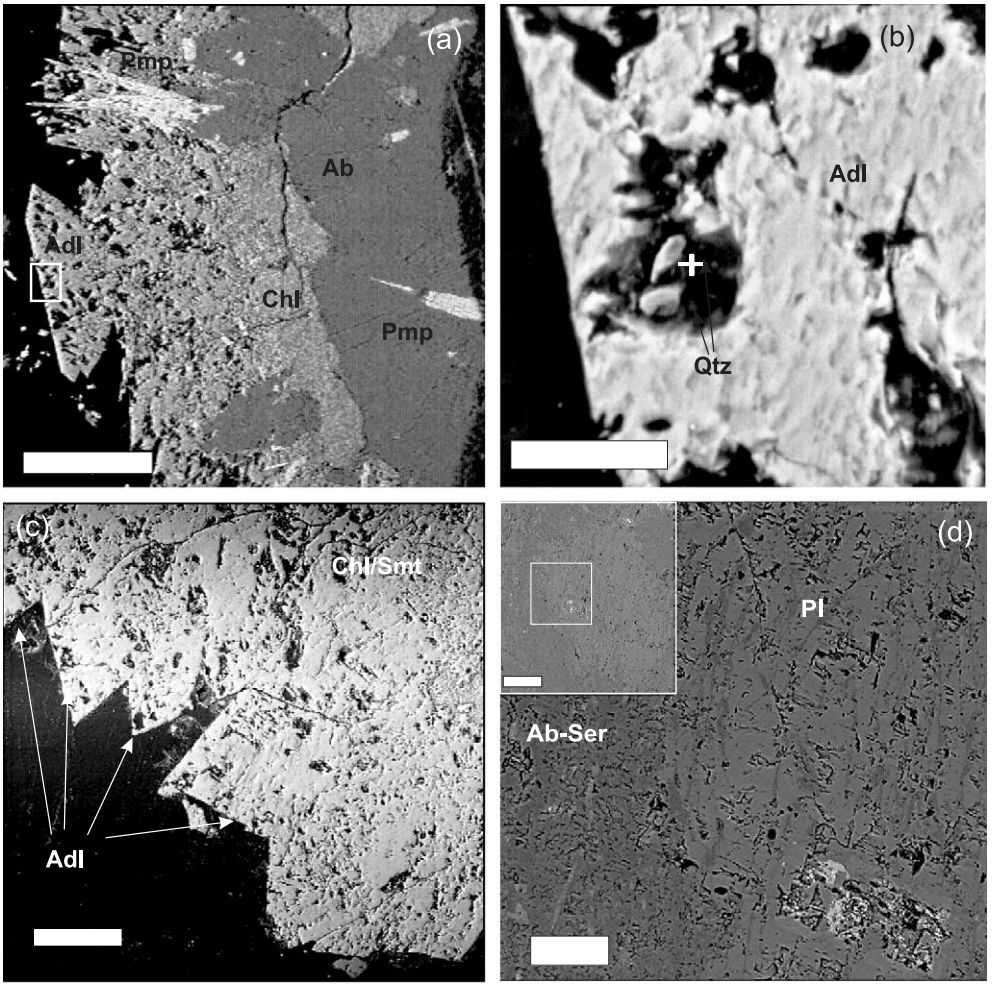

Fig. 3. Scanning electron micrograph (secondary electron images) of adularia in amygdales from lavas of the Chacana section. (a) Sample CHAC18, with adularia (Adl) in the inner part of an amygdale filled by pumpellyite (Pmp), chlorite (Chl) and an outer rim of albite (Ab). Scale bar=20 μ. (b) Detail of micropores in adularia from (a), with submicroscopic quartz (Qtz) inclusions. Scale bar=20 μ. (c) Adularia (Adl) filling amygdale with an outer rim of chlorite/smectite (Chl/Smt) in sample CHAC22. Scale bar=100 μ. (d) Detail of strongly sericitized plagioclase phenocryst (small inset, scale bar=200 μ) of sample CHAC8. Darker gray correspond to an fine intergrowth of albite-sericite (Ab-Ser) and light gray to plagioclase relic. Scale bar=50 μ.

Unit-cell dimensions of the adularias CHAC18 and CHAC22 were determined by least squares refinement of X-ray powder diffraction data using the program UnitCell of Holland and Redfern (1997). The X-ray data were treated as both monoclinic and triclinic and results are shown in Table 2. For both samples, the monoclinic and triclinic refinements gave proper solutions. However, for CHAC18, a triclinic adjustment appears more satisfactory, which using the conventional method of the b–c plot (Stewart and Wright, 1974; plot not shown) suggests the presence of subordinate albite, in accord with the X-ray powder diffraction pattern. Unit-cell dimensions for CHAC22 are slightly anomalous plotting outside the b–c quadrilateral. Two different features between both adularias can be distinctly identified. First, in terms of Al/Si ordering: CHAC18 adularia is relatively ordered, with $2t_1$=0.87 and t_1o+t_1m=0.84, whereas CHAC22 adularia is less ordered, with $2t_1$=0.79 and

Table 2
Results of refinement of X-ray powder diffraction data for adularias from the Chacana section of lava flows (central Chile)

Sample	System used for refinement	a (Å)	b (Å)	c (Å)	c^* (Å^{-1})	α (°)	β (°)	γ (°)	V (Å^3)	$2t_1$	t_1o+t_1m	Strain index
CHAC18	monoclinic	8.580±0.006	12.959±0.004	7.193±0.004	0.154613±0.000080		115.95±0.05		719.12±0.50	0.87		11.85
CHAC18	triclinic	8.581±0.005	12.967±0.004	7.197±0.003	0.154627±0.000071	90.10±0.04	116.03±0.04	89.87±0.04	719.56±0.46		0.84	7.26
CHAC22	monoclinic	8.566±0.006	12.987±0.006	7.208±0.003	0.154569±0.000087		116.16±0.05		719.73±0.49	0.79		−5.95
CHAC22	triclinic	8.566±0.006	12.986±0.008	7.208±0.004	0.154605±0.000110	90.00±0.10	116.19±0.07	89.92±0.10	719.49±0.85		0.78	−5.64

The parameters $2t_1$, t_1o+t_1m and strain index were calculated using Eqs. (5), (6) and (25), respectively, given in Kroll and Ribbe (1987).
The errors refer to one standard deviation and were estimated using the program UnitCell (Holland and Redfern, 1997).

$t_1o+t_1m=0.78$. Second, in terms of strain: CHAC18 adularia has a positive strain index (7.3–11.9%), whereas CHAC22 adularia has a negative strain index (−5.6 to −6.0%). This despite their compositions are close to pure $KAlSi_3O_8$ (strain index, in %, =0 for unstrained alkali feldspars, <0 for Na-rich strained phases and >0 for K-rich strained phases, Kroll and Ribbe, 1987). Strain in K-feldspar may result from unmixing of a Na-rich phase or substitution of Ca, Cs, B, Fe, NH^{4+} or H_3O^+ (Kroll and Ribbe, 1987). No major differences have been found between the chemistry of adularias from CHAC18 and those from CHAC22. However, the presence of quartz inclusions as revealed by SEM analyses (Fig. 3a and b) would confirm the existence of unmixed phases produced by crystallographic strain.

5. $^{40}Ar/^{39}Ar$ results

Results are summarized in Figs. 4–6, and Table 3.

6. Plagioclase ages

The plagioclase bulk sample separated from flow CHAC8 displayed a plateau age of 118.7±0.6 Ma (corresponding to 94.7% of ^{39}Ar released) whereas bulk sample from CHAC19 gave a U-shaped age spectrum characterized by disturbed apparent ages, around 110 Ma, at very low temperature, low apparent ages at intermediate temperatures of ca. 104 Ma and values close to 119 Ma at the highest temperatures (Fig. 4). The inverse isochron ($^{36}Ar/^{40}Ar$ vs. $^{39}Ar_K/^{40}Ar$) for CHAC8 (not shown) yields an age of 118.7±1.0 Ma (initial atmospheric $^{40}Ar/^{36}Ar$ ratio of 294.2±1.7, MSWD=2.1, Table 4). Small clusters of transparent plagioclase crystals from samples CHAC8, and CHAC19 displayed plateau ages of 114.7±2.0 and 117.0±1.1 Ma, respectively (Fig. 4). The inverse isochrons (not shown) give ages of 114.7±2.3 and 117.2±2.1 Ma (initial atmospheric $^{40}Ar/^{36}Ar$ ratio of 292.1±22.2 and 290.6±12.3, Table 4), respectively. The apparent ages of the two samples from CHAC19 converge at high temperature to 119 Ma.

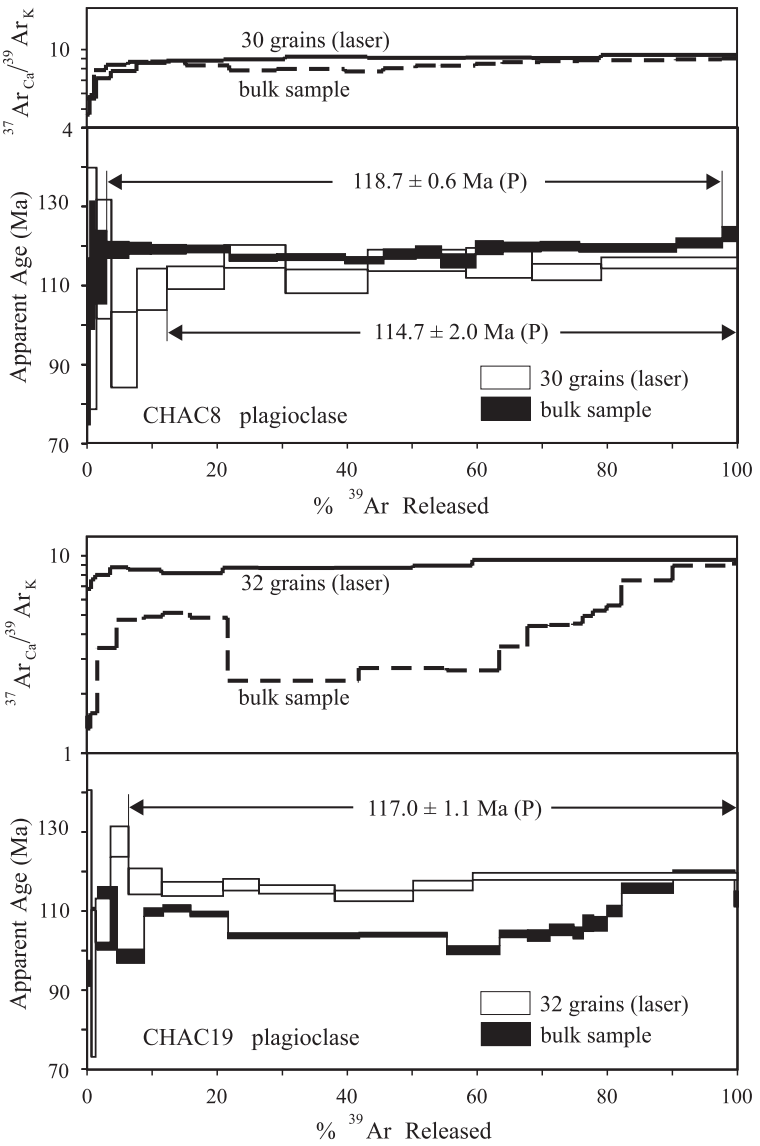

Fig. 4. $^{40}Ar/^{39}Ar$ age and $^{37}Ar_{Ca}/^{39}Ar_K$ ratio spectra obtained on two plagioclase bulk samples and two clusters of 30 and 32 grains of plagioclase from two lava flows (CHAC8 and CHAC19, respectively) from the Cordón de Chacana section. (P)=plateau age. Plateau ages are given at the 2σ level whereas the error bars for apparent ages are given at the 1σ level.

The $^{37}Ar_{Ca}/^{39}Ar_K$ ratio obtained from the gas fraction corresponding to: (i) the plateau ages from the cluster and the bulk sample of CHAC8 and (ii) the plateau age from the cluster and the high temperature age from the bulk sample of CHAC19 are around 8–9.5 (Fig. 4). EPMA analyses on fresh plagioclase phenocrysts of the same rock samples indicate that the corresponding $^{37}Ar_{Ca}/^{39}Ar_K$ ratios, calculated with the relationship $CaO/K_2O=2.179\times(^{37}Ar_{Ca}/^{39}Ar_K)$ (this relationship was not specifically calibrated for the corresponding irradiations, but was verified several times on several irradiations), with values of 10.09 ± 0.90 for CHAC8 and 10.00 ± 1.11 for CHAC19, approach the above ratios. This similarity, together with the tendency of apparent ages to converge at high temperature (Fig. 4), indicate that

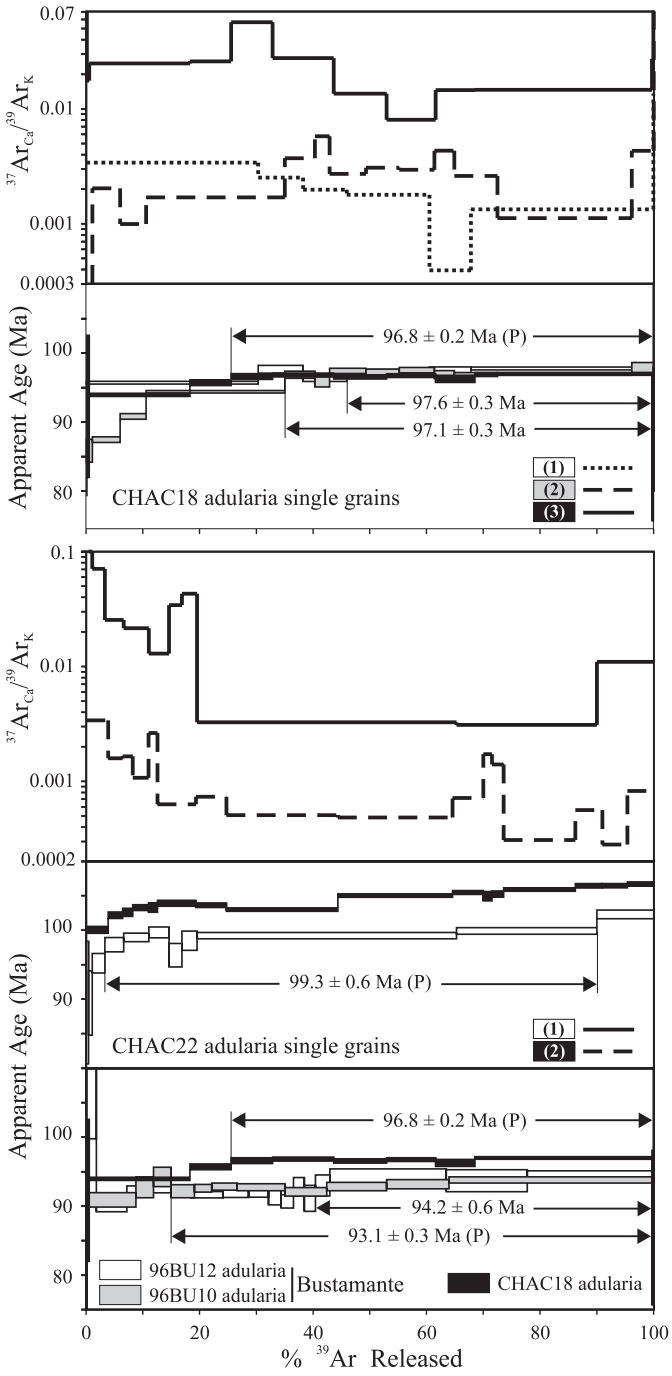

Fig. 5. $^{40}Ar/^{39}Ar$ age and $^{37}Ar_{Ca}/^{39}Ar_K$ ratio spectra obtained on single grains of adularia included in amygdales from two lava flows (CHAC18 and CHAC22) from the Cordón de Chacana section. The age spectra displayed by the adularias 96BU10 and 96BU12 from the Bustamante Hill section (Aguirre et al., 1999) are given for comparison with one adularia single grain of CHAC18. Ages not indicated by (P) are weighted mean ages. The numbers included in boxes are indicated in Tables 3 and 4. Same legend as Fig. 4.

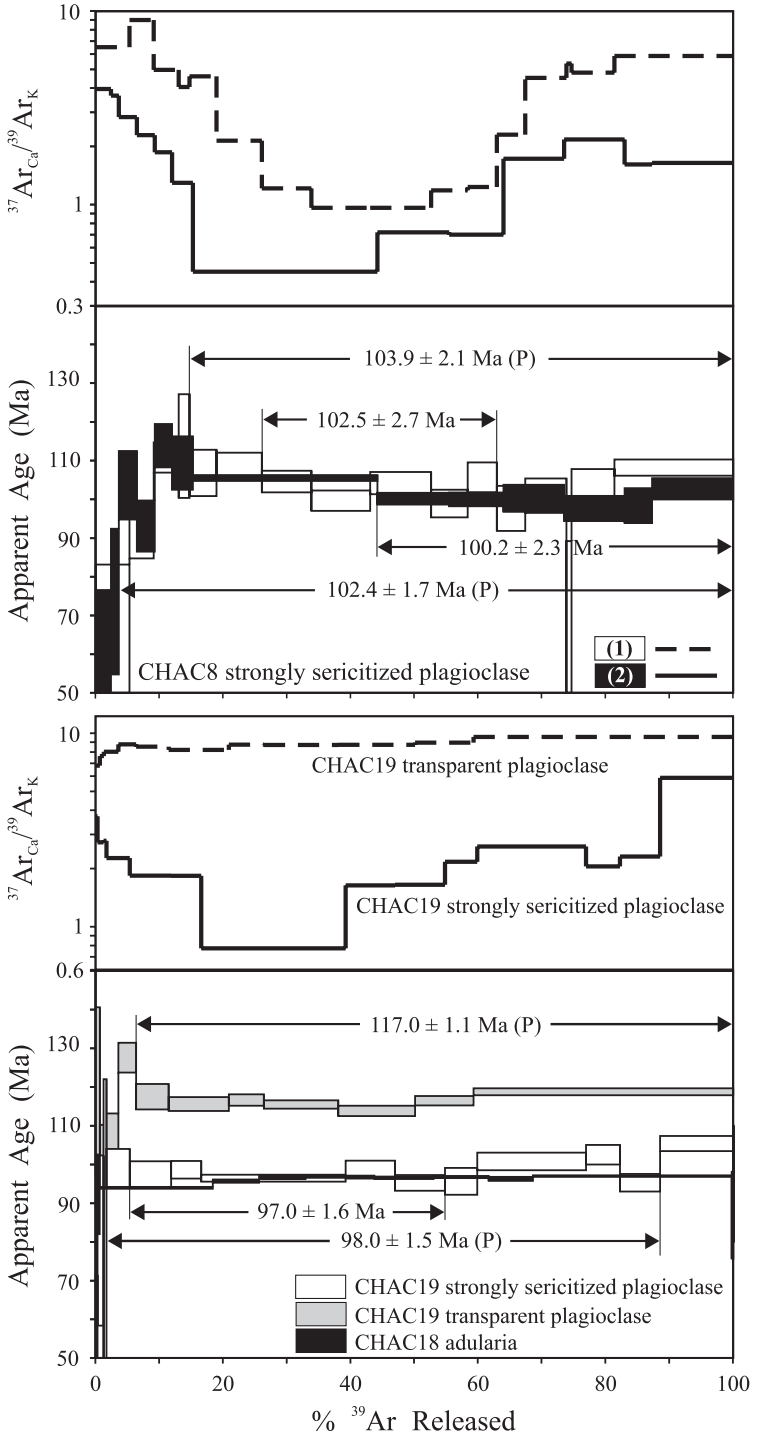

Fig. 6. $^{40}Ar/^{39}Ar$ age and $^{37}Ar_{Ca}/^{39}Ar_K$ ratio spectra obtained on single grains of strongly sericitized plagioclase from two lava flows (CHAC8 and CHAC19) from the Cordón de Chacana section. The age spectra displayed by one cluster of 32 grains of fresh plagioclase from CHAC19 lava flow (and the $^{37}Ar_{Ca}/^{39}Ar_K$ ratio spectrum) and one adularia single grain from CHAC18 lava flow are given for comparison. Same legend as Fig. 4.

Table 3
Detailed $^{40}Ar/^{39}Ar$ analytical results obtained on primary and metamorphic minerals from lava flows from the Cordón de Chacana (central Chile)

Temp. (°C) or step no.	Atmospheric contamination (%)	^{39}Ar (%)	$^{37}Ar_{Ca}/^{39}Ar_K$	$^{40}Ar^*/^{39}Ar_K$	Apparent age (Ma)±σ
CHAC8 plagioclase bulk sample, 41.8 mg (furnace heating) (J=0.01765)					
550	85.58	0.00	4.687	27.432	711.91±846.31
650	96.85	0.41	4.678	3.095	95.89±21.05
700	94.99	0.70	5.883	3.738	115.18±16.16
750	91.27	1.84	7.874	3.721	114.66±9.24
800	62.21	3.41	8.382	3.867	119.02±2.08
830	45.06	3.41	8.667	3.881	119.44±1.42
870	35.73	5.37	8.694	3.872	119.18±1.13
920	22.33	6.74	8.329	3.875	119.26±0.90
970	20.28	7.28	7.840	3.800	117.04±0.83
1020	17.45	10.47	7.983	3.806	117.22±0.78
1070	24.01	5.96	7.748	3.779	116.42±0.83
1120	42.78	4.96	8.061	3.831	117.95±1.24
1170	50.60	3.88	8.302	3.849	118.48±1.50
1220	58.88	5.32	8.289	3.775	116.27±1.73
1270	51.81	4.16	8.471	3.887	119.63±1.66
1320	43.78	5.80	8.628	3.892	119.76±1.16
1370	37.19	5.97	8.737	3.899	119.98±1.12
1420	35.13	14.90	8.837	3.884	119.53±1.01
1470	33.86	7.07	8.934	3.927	120.82±1.19
Fuse	28.34	2.35	9.029	4.001	123.03±1.83
					Integrated age=118.58±0.37 Ma
CHAC8 plagioclase 30 grains (laser heating) (J=0.01765)					
1	87.93	1.42	5.662	3.538	109.27±30.55
2	57.85	2.28	7.184	3.786	116.68±15.06
3	39.11	3.96	7.812	3.024	93.78±9.56
4	16.89	4.61	8.593	3.531	109.06±5.25
5	14.64	8.79	8.795	3.630	112.00±2.88
6	11.91	9.42	8.948	3.810	117.38±2.89
7	18.54	12.65	9.230	3.599	111.10±3.02
8	17.81	15.15	9.093	3.775	116.36±2.71
9	11.06	10.16	9.121	3.755	115.75±3.80
10	10.79	10.63	9.079	3.676	113.40±2.08
Fuse	10.05	20.94	9.433	3.755	115.74±1.38
					Integrated age=113.61±1.11 Ma
CHAC19 plagioclase bulk sample, 50.5 mg (furnace heating) (J=0.01765)					
450	147.66	0.00	7.921	−79.018	0.00±0.00
550	99.11	0.07	1.547	0.683	21.63±29.93
650	91.17	0.49	1.332	3.210	99.46±8.42
700	85.64	1.05	1.593	3.413	105.57±5.29
750	90.38	2.97	3.411	3.499	108.16±7.97
800	58.76	4.18	4.729	3.180	98.56±1.72
830	37.01	2.91	4.917	3.553	109.78±0.99
870	35.23	4.19	5.130	3.584	110.71±0.84
920	23.70	5.79	4.857	3.536	109.27±0.64
970	25.64	20.16	2.325	3.353	103.76±0.66
1010	21.59	13.51	2.698	3.362	104.04±0.51
1040	30.34	8.11	2.620	3.232	100.12±1.05

(continued on next page)

Table 3 (*continued*)

Temp. (°C) or step no.	Atmospheric contamination (%)	^{39}Ar (%)	$^{37}Ar_{Ca}/^{39}Ar_K$	$^{40}Ar^*/^{39}Ar_K$	Apparent age (Ma)±σ
CHAC19 plagioclase bulk sample, 50.5 mg (furnace heating) (J=0.01765)					
1070	41.28	4.33	3.471	3.369	104.24±0.88
1100	54.59	3.40	4.411	3.354	103.80±1.39
1130	56.03	3.63	4.465	3.403	105.28±1.40
1160	55.11	1.47	4.532	3.377	104.47±1.42
1190	54.28	1.57	4.957	3.460	106.97±2.01
1240	55.08	2.12	5.276	3.454	106.79±1.78
1290	52.57	2.27	5.588	3.562	110.03±1.36
1360	43.99	7.86	7.505	3.754	115.79±1.22
1430	37.42	9.46	8.913	3.871	119.26±1.10
Fuse	39.47	0.46	9.317	3.663	113.06±1.93
					Integrated age=106.93±0.36 Ma
CHAC19 plagioclase 32 grains (laser heating) (J=0.01765)					
1	90.15	0.67	6.794	3.864	119.05±21.58
2	84.92	0.63	7.597	2.952	91.67±18.57
3	73.34	2.28	7.992	3.481	107.61±5.57
4	26.14	2.79	8.743	4.151	127.61±3.84
5	25.13	5.09	8.511	3.812	117.53±3.29
6	24.45	9.42	8.183	3.748	115.59±1.79
7	14.90	5.51	8.701	3.784	116.68±1.48
8	18.92	11.66	8.667	3.745	115.50±1.07
9	21.37	12.09	8.680	3.689	113.85±1.33
10	25.15	9.16	8.923	3.778	116.49±1.24
Fuse	18.48	40.71	9.531	3.855	118.79±0.89
					Integrated age=116.94±0.56 Ma
CHAC18 adularia single grain (1) (laser heating) (J=0.01765)					
1	0.26	30.28	0.003	3.085	95.73±0.21
2	0.14	7.91	0.003	3.149	97.67±0.57
3	1.30	7.75	0.002	3.104	96.31±0.40
4	0.41	14.55	0.002	3.137	97.32±0.34
5	0.31	7.30	0.000	3.144	97.51±0.52
6	3.58	32.14	0.001	3.153	97.79±0.22
Fuse	70.19	0.07	0.014	1.036	32.73±56.33
					Integrated age=96.91±0.13 Ma
CHAC18 adularia single grain (2) (laser heating) (J=0.01765)					
1	3.73	1.08	0.000	2.759	85.87±1.66
2	1.92	4.87	0.002	2.812	87.46±0.41
3	0.41	4.59	0.001	2.923	90.84±0.41
4	0.43	24.43	0.002	3.041	94.41±0.18
5	0.48	5.30	0.004	3.123	96.88±0.52
6	1.60	2.59	0.006	3.088	95.84±0.73
7	0.56	6.43	0.003	3.142	97.45±0.38
8	0.64	5.89	0.003	3.136	97.29±0.43
9	0.13	6.17	0.003	3.145	97.55±0.40
10	0.89	3.51	0.004	3.123	96.90±0.59
11	1.12	7.60	0.003	3.124	96.91±0.29
12	2.82	23.65	0.001	3.127	97.01±0.20

Table 3 (*continued*)

Temp. (°C) or step no.	Atmospheric contamination (%)	^{39}Ar (%)	$^{37}Ar_{Ca}/^{39}Ar_K$	$^{40}Ar^*/^{39}Ar_K$	Apparent age (Ma)±σ
CHAC18 adularia single grain (2) (laser heating) (J=0.01765)					
13	10.88	3.88	0.004	3.157	97.93±0.74
Fuse	0.00	0.01	0.276	5.599	170.17±298.10
					Integrated age=95.58±0.10 Ma
CHAC18 adularia single grain (3) (laser heating) (J=0.00637)					
1	35.75	0.12	0.439	5.113	57.81±21.45
2	0.00	0.40	0.018	8.243	92.30±10.30
3	0.67	17.74	0.025	8.395	93.96±0.24
4	0.46	7.27	0.026	8.556	95.72±0.42
5	0.00	7.28	0.057	8.639	96.62±0.42
6	0.37	10.77	0.028	8.659	96.84±0.29
7	0.96	9.37	0.014	8.635	96.57±0.31
8	0.74	8.62	0.008	8.651	96.75±0.27
9	1.21	6.92	0.015	8.608	96.28±0.51
10	9.12	31.19	0.015	8.674	97.00±0.18
11	31.38	0.24	0.027	7.749	86.90±11.20
Fuse	17.12	0.08	0.293	9.980	111.17±31.15
					Integrated age=96.13±0.12 Ma
CHAC22 adularia single grain (1) (laser heating) (J=0.00637)					
1	79.29	0.40	0.410	7.989	89.50±8.88
2	41.39	0.67	0.190	7.984	89.44±4.66
3	12.69	2.21	0.071	8.512	95.20±1.42
4	14.14	3.32	0.025	8.760	97.91±1.04
5	14.43	4.43	0.022	8.857	98.96±0.62
6	13.06	3.55	0.013	8.924	99.69±0.78
7	22.71	2.26	0.034	8.620	96.38±1.70
8	16.85	2.65	0.043	8.813	98.48±1.39
9	42.14	45.76	0.003	8.880	99.22±0.46
10	42.98	24.71	0.003	8.943	99.89±0.47
Fuse	41.12	10.03	0.011	9.164	102.30±0.62
					Integrated age=99.38±0.27 Ma
CHAC22 adularia single grain (2) (laser heating) (J=0.01765)					
1	17.77	3.84	0.003	3.230	100.05±0.49
2	2.40	2.55	0.002	3.300	102.18±0.46
3	4.83	1.79	0.002	3.314	102.59±0.58
4	0.65	2.82	0.001	3.337	103.28±0.42
5	1.00	1.54	0.003	3.337	103.29±0.69
6	22.75	6.80	0.001	3.358	103.91±0.44
7	6.12	5.34	0.001	3.348	103.63±0.32
8	10.30	19.63	0.001	3.328	103.00±0.26
9	7.02	20.25	0.000	3.395	105.03±0.26
10	4.59	5.41	0.001	3.410	105.47±0.27
11	5.82	1.53	0.002	3.392	104.94±0.67
12	6.44	2.08	0.001	3.402	105.24±0.45
13	4.70	12.61	0.000	3.424	105.91±0.25
14	3.92	4.76	0.001	3.442	106.45±0.31

(continued on next page)

Table 3 (*continued*)

Temp. (°C) or step no.	Atmospheric contamination (%)	^{39}Ar (%)	$^{37}Ar_{Ca}/^{39}Ar_K$	$^{40}Ar^*/^{39}Ar_K$	Apparent age (Ma)±σ
CHAC22 adularia single grain (2) (laser heating) (J=0.01765)					
15	5.73	4.42	0.000	3.443	106.47±0.31
Fuse	6.26	4.65	0.001	3.451	106.70±0.30
					Integrated age=104.44±0.10 Ma
CHAC8 strongly sericitized plagioclase (1) (laser heating) (J=0.01765)					
1	99.42	5.31	6.510	1.098	34.62±48.53
2	81.35	3.81	8.991	2.972	92.23±7.44
3	34.35	3.90	4.967	3.591	110.84±3.93
4	25.21	1.71	4.051	3.690	113.80±13.40
5	29.19	4.23	4.596	3.457	106.85±5.96
6	21.48	7.11	2.141	3.520	108.73±3.33
7	25.60	7.77	1.212	3.383	104.63±2.78
8	27.99	9.23	0.964	3.218	99.65±2.62
9	23.99	9.56	0.963	3.370	104.21±2.87
10	30.35	5.75	1.185	3.195	98.95±3.55
11	28.23	4.57	1.236	3.419	105.69±3.86
12	45.32	4.44	2.300	3.153	97.69±5.83
13	63.58	6.47	4.520	3.262	100.96±4.45
14	77.50	0.80	5.356	2.115	66.10±23.13
15	62.86	6.73	4.806	3.376	104.39±3.46
Fuse	55.34	18.60	5.868	3.503	108.22±2.13
					Integrated age=100.32±2.67 Ma
CHAC8 strongly sericitized plagioclase (2) (laser heating) (J=0.01765)					
1	98.58	2.40	3.957	1.718	53.88±22.73
2	93.09	1.24	3.656	2.360	73.61±18.82
3	74.82	2.83	2.833	3.351	103.66±8.86
4	62.24	2.80	2.285	3.001	93.08±6.57
5	39.30	2.73	1.864	3.692	113.86±5.59
6	35.08	3.25	1.296	3.542	109.38±6.89
7	36.67	28.94	0.451	3.414	105.53±0.76
8	34.85	11.28	0.719	3.235	100.16±1.51
9	37.19	8.51	0.699	3.230	100.00±1.76
10	61.64	9.51	1.726	3.240	100.30±3.49
11	73.09	9.47	2.171	3.152	97.66±3.27
12	67.16	4.32	1.615	3.177	98.42±4.52
Fuse	60.93	12.71	1.643	3.321	102.74±2.75
					Integrated age=100.88±0.99 Ma
CHAC19 strongly sericitized plagioclase (laser heating) (J=0.01765)					
1	98.70	0.30	3.724	0.554	17.55±53.99
2	90.93	0.94	2.735	2.580	80.38±21.97
3	74.40	0.49	2.782	2.641	82.23±39.81
4	80.48	3.64	2.264	3.196	99.03±5.00
5	52.77	6.45	1.837	3.146	97.52±3.33
6	31.35	4.76	1.833	3.183	98.65±2.28
7	38.73	22.63	0.774	3.112	96.49±0.89
8	30.21	7.77	1.638	3.185	98.70±2.32

Table 3 (*continued*)

Temp. (°C) or step no.	Atmospheric contamination (%)	^{39}Ar (%)	$^{37}Ar_{Ca}/^{39}Ar_K$	$^{40}Ar^*/^{39}Ar_K$	Apparent age (Ma)±σ
CHAC19 strongly sericitized plagioclase (laser heating) (J=0.01765)					
9	35.44	7.84	1.649	3.071	95.27±2.04
10	43.18	5.06	2.169	3.084	95.67±3.48
11	58.41	17.06	2.599	3.255	100.80±2.29
12	49.19	5.34	2.050	3.313	102.55±2.52
13	55.53	6.26	2.308	3.072	95.30±2.26
Fuse	48.09	11.45	5.887	3.409	105.44±1.96
					Integrated age=98.35±0.75 Ma

Step=temperature (°C) or step number for the sample analyzed with a furnace system or a laser probe, respectively. $^{40}Ar^*$=radiogenic ^{40}Ar. Ca and K=produced by Ca and K neutron interference, respectively. *J*=irradiation parameter. The error is at the 1σ level and does not include the error in the value of the *J* parameter. Age calculations are made using the decay constants given by Steiger and Jäger (1977). The numbers within brackets following some of the sample numbers are indicated in Figs. 5 and 6. Correction factors for interfering isotopes were $(^{39}Ar/^{37}Ar)_{Ca}=7.06\times10^{-4}\pm4\%$, $(^{36}Ar/^{37}Ar)_{Ca}=2.79\times10^{-4}\pm4\%$ and $(^{40}Ar/^{39}Ar)_K=2.97\times10^{-2}\pm2\%$.

the plateau ages correspond to analyses of fresh plagioclase and therefore probably represent the crystallisation ages of the lava flows. For the sample CHAC8, because of the higher quality of data mainly due to much higher Ar signals, the plateau age obtained on the bulk sample is preferred.

7. Adularia ages

Three single crystals of adularia from CHAC18 displayed age spectra characterized by a variable increase of apparent ages at low temperatures followed by a flat region at the intermediate and high temperature steps (Fig. 5). One plateau age at 96.8±0.2 Ma (corresponding to 74% of ^{39}Ar released) is obtained, close to weighted mean ages of 97.6±0.3 and 97.1±0.3 Ma, displayed by three to nine concordant successive apparent ages displayed by the two other grains (corresponding to 54% and 65% of total released ^{39}Ar, respectively). The isochron plots (not shown) give ages of 96.6±0.4, 95.9±0.9 and 97.0±0.5 Ma, with initial $^{40}Ar/^{36}Ar$ ratios poorly defined. The corresponding $^{37}Ar_{Ca}/^{39}Ar_K$ ratios appear variable, but lower than 0.06, probably approaching the composition of pure adularia (Fig. 5). EPMA analyses gave CaO/K_2O ratios ranging from 0.000 up to 0.001, which confirm the validity of this assumption. Two single grains of adularia from CHAC22 yield discordant age spectra with steadily increasing apparent ages (Fig. 5) and a plateau age at 99.3±0.6 Ma. For comparison, the age spectra of two adularia crystals from the Bustamante section (samples 96BU10-12 in Aguirre et al., 1999) are represented in Fig. 5. The plateau ages are significantly different in the two locations.

8. Altered plagioclase ages

Under the SEM, the cloudy and strongly altered plagioclase crystals can be described as consisting mainly of a cryptocrystalline intergrowth of albite and sericite with the sericite richest parts appearing as discrete islets. Minute and scarce microdomains of plagioclase, richer in Ca as compared with albite, are also present (Fig. 3d).

Two of these single plagioclase crystals from CHAC8 gave disturbed age spectra with more or less saddle shapes (after increasing ages at low temperature), but showing plateau ages of 102.4±1.7 and 103.9±2.1 Ma (Fig. 6). The inverse isochrons display concordant ages of 105.6±3.4 and 102.3±3.8 Ma, respectively. One single grain of sericitized plagioclase from CHAC19 displayed a plateau age of 98.0±1.5 Ma and a slightly lower weighted mean age of 97.0±1.6 Ma at intermediate temperature, corresponding to the lowest $^{37}Ar_{Ca}/^{39}Ar_K$ ratio (Fig. 6), ca. to the maximum degasing of the sericite. The isochron age is 96.3±2.3 Ma on the plateau age

Table 4
Summary of $^{40}Ar/^{39}Ar$ data of primary and metamorphic minerals from the Chacana section of lava flows (central Chile)

Sample (*location*)	Material	Integrated age (Ma)	Plateau age (Ma)	w.m.a. (Ma)	Steps in the plateau or w.m.a.	$\%^{39}Ar$ in the plateau or w.m.a.	Inverse isochron age (Ma)	Steps in the inverse isochron	$(^{40}Ar/^{36}Ar)_i$	MSWD
CHA8 (*0306746/6385949*)	plagioclase bulk sample	118.6±0.7	118.7±0.6		800–1470	94.7	118.7±1.0	550–1470	294.2±1.7	2.1
CHAC8	plagioclase 30 grains	113.6±2.2	114.7±2.0		5-fuse	87.7	114.7±2.3	1-fuse	292.1±22.2	1.1
CHAC19 (*0308608/6388929*)	plagioclase bulk sample	106.9±0.7					106.8±2.8	450-fuse	295.3±7.6	29.4
CHAC19	plagioclase 32 grains	116.9±1.1	117.0±1.1		5-fuse	93.6	117.2±2.1	1-fuse	290.6±12.3	2.4
CHAC18 (*0308603/6388329*)	adularia (1) single grain	96.9±0.3		97.6±0.3	4–6	54.0	95.9±0.9	1–6	451.3±58.8	3.4
CHAC18	adularia (2) single grain	95.6±0.2		97.1±0.3	5–13	65.0	97.0±0.5	5–13	310.5±37.4	0.8
CHAC18	adularia (3) single grain	96.1±0.2	96.8±0.2		5–10	74.2	96.6±0.4	5–12	305.9±8.6	0.3
CHAC22	adularia (1) single grain	99.4±0.5	99.3±0.6		4–10	86.7	98.2±1.5	3–10	300.9±7.3	1.7
CHAC22 (*0309040/6388467*)	adularia (2) single grain	104.4±0.2					105.3±1.4	1-fuse	272.8±35.4	23.6
CHAC8	strongly sericitized plagioclase (1) single grain	100.3±5.3	103.9±2.1		5-fuse	85.3	102.3±3.8	7–15	295.2±12.4	1.1
CHAC8	strongly sericitized plagioclase (2) single grain	100.9±2.0	102.4±1.7		3-fuse	96.4	105.6±3.4	3-fuse	287.6±10.9	2.7
CHAC19	strongly sericitized plagioclase single grain	98.4±1.5	98.0±1.5		4–13	86.8	96.3±2.3	4–13	299.2±7.2	1.0

Step=temperature (°C) or step number for the sample analysed with a furnace system or a laser probe, respectively. w.m.a.=weighted mean age. $(^{40}Ar/^{36}Ar)_i$=initial ratio from inverse isochron. The errors are quoted at the 2σ level. The inverse isochron $(^{40}Ar/^{36}Ar)_i$ ratio and age are calculated from the best-fit line (York, 1969). The errors are taken as the 95% confidence limit of York's model-1 fit. MSWD=mean square of weighted deviates=SUMS/($n-2$), with SUMS=minimum weighted sum of residuals and n=number of points fitted. The numbers within brackets following some of the materials are indicated in Figs. 5 and 6. The GPS coordinates of the samples are indicated (projection South America 56).

fraction. At high temperature, the apparent ages are slightly increasing probably because of progressive degasing of the unaltered plagioclase, as shown by increasing $^{37}Ar_{Ca}/^{39}Ar_K$ ratio. When we plot the apparent ages obtained on CHAC 19 versus the $^{37}Ar_{Ca}/^{39}Ar_K$ ratio (Fig. 7), we observe a regular increasing of ages with $^{37}Ar_{Ca}/^{39}Ar_K$ ratio, whatever the type of analyzed plagioclase (fresh or strongly sericitized). The most regular trend is given by the bulk sample that represents a mixture of fresh and altered minerals. It clearly appears from all data that the fractions approaching the composition of pure plagioclase (ratio around 10 measured with microprobe) converge to 118–120 Ma, whereas fractions corresponding to the highest proportions of sericite in plagioclase display the youngest ages around 95–100 Ma. In conclusion, when compared to the CHAC18 adularia plateau age (96.8±0.2 Ma), it is likely that

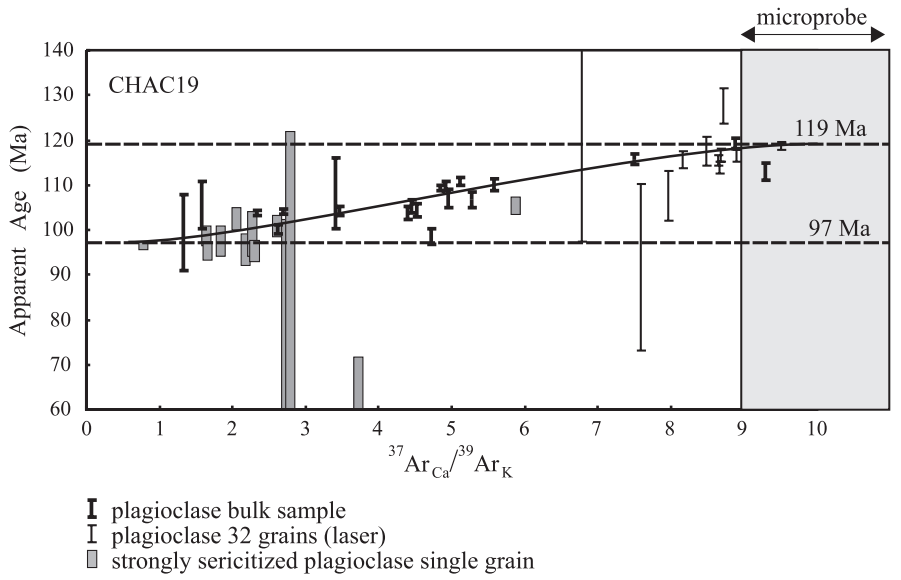

Fig. 7. $^{40}Ar/^{39}Ar$ apparent ages versus the $^{37}Ar_{Ca}/^{39}Ar_K$ ratio obtained on plagioclase bulk samples, clusters of grains of plagioclase and single grains of strongly sericitized plagioclase from the lava flow CHAC19 from the Cordón de Chacana section. In grey is indicated the $^{37}Ar_{Ca}/^{39}Ar_K$ ratio deduced from the Ca/K ratio measured on fresh plagioclase with the microprobe. The two ages of 119 and 97 Ma, corresponding to fresh plagioclase (high temperature age of CHAC19 and plateau age of CHAC8) and adularia plateau age of CHAC18, respectively, are indicated by dashed lines.

the weighted mean age of 97.0±1.6 Ma represents the best estimate of the age of the sericite included into plagioclase.

9. Discussion

Whereas one (CHAC8) of the analyzed fresh plagioclases gives undisturbed age spectra on both bulk sample and small grain cluster (heated with laser), CHAC19 displays a plateau age only on small grain cluster, and the bulk sample shows the existence of altered phases as sericite, that could not be eliminated even during a careful mineral separation. The most precise plateau age of 118.7±0.6 Ma (CHAC8) is similar to the plateau ages displayed by the fresh plagioclase from the Bustamante Hill section (119.4±2.4 (2σ) Ma: Aguirre et al., 1999). For CHAC19, despite the existence of a plateau age (117.0±1.1 Ma), the high temperature ages of about 119 Ma obtained on both bulk sample and small grain cluster more probably represent the best age estimate of this rock, because they correspond to purer igneous plagioclase.

The analyzed plagioclase phenocrysts are free of albitization and keep their primitive calcic composition (CHAC8: $An_{58–55}Ab_{39–42}Or_3$, CHAC-19: $An_{58–55}Ab_{39–42}Or_3$). Metamorphic temperatures obtained from chlorites (47 analyses in 7 different samples) give a mean value of 239 °C. In the Veta Negra Formation, the metamorphic grade is in the prehnite-pumpellyite facies for which the temperature range is 170–280 °C according to the petrogenetic grid of Frey et al. (1991). Absence of actinolite or zeolite in the associations studied in Bustamante and Chacana sections fits with the metamorphic temperature value (239 °C) given by the chlorite geothermometry. Although the closure temperature of plagioclase is not precisely known, the estimated metamorphic temperature domain of these rocks and the fact that the age spectra do not show any evidence of thermal disturbance, the plateau ages displayed by transparent plagioclases probably reflect the emplacement of the lava flows and not a reseting of the K/Ar system (that should be complete) due to metamorphic conditions.

Adularia single grains from one lava flow (CHAC18) display clustered high temperature ages (including one plateau age), whereas adularia from

one other rock (CHAC22) gives variable ages (including one plateau age slightly older than CHAC18). This difference of behaviour of adularia from these two lava flows is not related to chemistry (Table 1) but could be a consequence of the different Al/Si ordering and strain indexes measured by X-ray diffraction (Table 2). As previously proposed by McDougall and Harrison (1999), unmixing and reordering in K-feldspars may affect the argon retentivity. Reordering in unaltered adularias is mainly controlled by the process of primary crystal growth (Dong and Morrison, 1995), so that the different behaviour of the K/Ar chronometer in CHAC18 and CHAC22 could be explained by different strain indexes (see Table 2). The reproducibility of results obtained on CHAC18 represents a strong argument to consider the corresponding plateau age as geologically significant. This age at 96.8±0.2 Ma may be considered as representing the metamorphic event since this mineral is part of low-variance equilibrium assemblages (Fig. 3a) in amygdale metadomains.

The strongly sericitized plagioclase ages obtained on CHAC19 and corresponding to the lowest Ca/K ratios, that represent the gas fractions most enriched in sericite, fall in the same adularia interval: both the plateau age at 98.0±1.5 Ma and the weighted mean at 97.0±1.6 Ma (Fig. 6) are concordant with the CHAC18 adularia plateau age. This result (1) demonstrates that valid ages may be obtained on sericite by analyzing strongly sericitized plagioclase single grains (the plagioclase radiogenic component appears as negligible in that case) and (2) confirms the fact already pointed out by Morata et al. (1997) that sericite and albite, although present in a different metadomain with respect to adularia, are part of the main metamorphic paragenesis. Fig. 7 clearly shows an ideal example of a plagioclase (CHAC19) consisting of a simple mixture between pure plagioclase and pure sericite.

For the sample CHAC8 that is located about 1000 m below CHAC19 in the stratigraphic pile, we get slightly higher plateau ages (103.9±2.1 and 102.4±1.7 Ma). Nevertheless, intermediate to high temperature gas fractions display slightly lower ages of 102.5±2.7 and 100.2±2.3 Ma (respectively) (Fig. 6) that are probably more representative of the age of sericite. However, the relationship between apparent ages and the $^{37}Ar_{Ca}/^{39}Ar_{K}$ ratio is not so clear in this sample as it is in sample CHAC 19 (Fig. 6), this might be the result of a more complex composition of the alteration minerals in the case of CHAC8. In fact, as observed on thin sections, the crystals of strongly sericitized plagioclase from CHAC8 present more chlorite and chlorite/smectite patches than those in sample CHAC19. This may disturb the K/Ar system of the plagioclase without decreasing the $^{37}Ar_{Ca}/^{39}Ar_{K}$ ratio. Unfortunately, the real mineralogical composition of the strongly altered plagioclase single grains that are step heated cannot be determined. Although the slight age (but within error bars) difference between CHAC19 (97.0±1.6 Ma) and CHAC8 (102.5±2.7 and 100.2±2.3 Ma) sericitized plagioclases is in agreement with their respective stratigraphic position, an eventual diachronic sericite crystallisation along the stratigraphic sequence must be confirmed by more precise data. The temperature of crystallisation of sericite, that may be deduced from the crystallisation temperature of cogenetic chlorite (on the order of 260–280 °C, calculated), is here probably lower than its closure temperature, estimated around 350°C, as muscovite.

The age of metamorphism found for the Cordón de Chacana (around 97 Ma, from the best age data obtained on CHAC19) is slightly older than that of the Bustamante Hill (adularia: 93–94 Ma) (Fig. 5) in contrast with the volcanic ages that precisely coincide in the two areas (ca. 119 Ma). Consequently, the time interval between the volcanic and the metamorphic event at the Cordón de Chacana is slightly shorter (22 Ma) than the one obtained at the Bustamante Hill (ca. 25 Ma, Aguirre et al., 1999). These last authors proposed that this metamorphism was the result of burial conditions only, mainly because the metamorphic gradient is clearly related to the stratigraphic depth of the lava flows and not to the distance to the intrusives. Nevertheless, more recently, the first $^{40}Ar/^{39}Ar$ precise dating of one (Caleu pluton) of the well developed intrusive bodies of the region (Fig. 1) displayed ages ranging from 94.9±1.8 to 93.2±1.1 Ma on amphibole, biotite and plagioclase (Parada et al., in press). These ages are coeval with adularia ages from the Bustamante Hill and slightly younger than adularia and sericite from the Cordón de Chacana. Moreover, the ages of the Caleu pluton are in close agreement with K/Ar ages reported for other Creta-

ceous plutons, e.g.: (i) granitoid about 3 km to the north of the Bustamante Hill (91±2 (2σ) and 96±2 Ma both obtained on biotites: Wall et al., 1999), (ii) granitoid about 20 km to the north of the Bustamante Hill (94±2 and 96±2 Ma obtained also on biotites: Wall et al., 1999) and (iii) diorite about 21 km to the north of the Cordón de Chacana (92±3 and 96±3 Ma both obtained on whole rocks: Rivano et al., 1993). Consequently, it appears clearly that the metamorphism affecting the Veta Negra Formation is due to the additional effect of both the burial conditions and one (or more?) anomalous thermal gradient related to a regional magmatic event at the origin of the intrusives. Nevertheless, more precise age data are necessary to know if more than one distinct thermal event affected the Veta Negra Formation.

The age of the metamorphism found in the Cordón de Chacana area is slightly younger than the $^{40}Ar/^{39}Ar$ ages displayed by K-feldspars (microcline and orthoclase) related to the mineralizations of the nearby strata-bound El Soldado copper deposit (Fig. 1), emplaced in volcanic rocks of the uppermost levels of the Lo Prado Formation (Wilson et al., 2003). These ages, ranging from 100.5±1.5 to 106.1±1.1 Ma, are interpreted by these authors as representing an hydrothermal event (at the origin of the copper deposits) that followed a burial metamorphic episode in the zeolite facies, occurring at about 110 Ma (age of the oldest K-feldspars apparently not related to mineralizations). Our data obtained on metamorphic minerals from the Cordón de Chacana (about 97 Ma) and the Bustamante Hill (around 94 Ma, Aguirre et al., 1999), were obtained from lava flows of the central part of the Veta Negra Formation, stratigraphically higher than the El Soldado host rocks (estimated stratigraphic depth difference=3000 m) (see Fig. 2). If these ages reflect a regular basinal subsidence process, we can estimate the subsidence rate by comparing ages obtained from very low grade metamorphic K-feldspars from El Soldado and Cordón de Chacana. If the measured ages correspond to crystallisation ages of the K-feldspars (on the order of 250 °C), the difference of both ages (13 Ma) and of the stratigraphic depths (ca. 3000 m) would allow to calculate a subsidence rate of about 0.24 mm/year. This value is fairly close to the subsidence rate of >0.25 and 0.15–0.18 mm/year for the intra-arc basin of the Coastal Range of central Chile during the early Cretaceous advocated by Vergara et al. (1995) and Aguirre et al. (1999), respectively.

This apparent increase of ages on very low-grade minerals with stratigraphic depth and the converging subsidence rates are in agreement with the development of burial-type metamorphism in the extensional setting proposed for the early Cretaceous intra-arc basin of the Coastal Range of central Chile. The rocks of the Lo Prado Formation at the strata-bound El Soldado copper deposit and of the Veta Negra Formation have been affected by the same non-deformative metamorphism in the prehnite-pumpellyite facies. Consequently, the counter-clockwise *P–T–t* path for the metamorphism of the early Cretaceous rocks of central Chile proposed by Aguirre et al. (1989) should have travelled inside the prehnite-pumpellyite facies domain between ca. 97 and 110 Ma. Nevertheless, it remains to clarify the relative influence of thermal events relatively to a simple burial process during the subsidence history of the intra-arc basins.

10. Conclusions

(1) Apparently valid ages of both the emplacement of lava flows (by dating transparent plagioclase) and their subsequent very low-grade metamorphic event (by dating sericite and/or adularia) were measured on the same lava series, and even on the same rock sample (CHAC19). Sericite, extensively developed in altered basalts, could be dated by analysing single grains of strongly altered plagioclase. The validity of this age is demonstrated by concordant ages obtained on adularia.

(2) The age of ca. 119 Ma obtained for the non-sericitized plagioclase crystals of CHAC8 and CHAC19 is probably the age of emplacement of the studied lava flows from the Cordón de Chacana area. The coincidence of this age with the one obtained for the flows at the Bustamante Hill area, located in the Santiago region (Aguirre et al., 1999), may indicate that the volcanic activity of the Veta Negra Formation was synchronous along the 80-km long latitudinal segment studied.

(3) Because adularia and sericite belong to the same very low-grade metamorphic paragenesis, the

age of 97 Ma obtained on both secondary minerals represents the age of this metamorphism. It appears slightly older than the ages measured on adularia in the Bustamante Hill area (93–94 Ma). These last ages may be the result of the combined effect of burial metamorphism and a high thermal regional gradient related to the emplacement of well-developed plutons. The time interval between volcanism and metamorphism is about 22 Ma at Cordón de Chacana, slightly shorter than in the Bustamante Hill region.

(4) We observe an apparent age gradient on very low-grade minerals (adularia and/or sericite) between Cordón de Chacana and El Soldado rocks (about 3000 m below; Wilson et al., 2003). Despite (i) some large error bars on ages of strongly sericitized plagioclase and (ii) the different locations of the studied formations, this age gradient may outline the significant effect of burial relatively to the contribution of high thermal gradient event(s). More age data are necessary to correctly differentiate these two effects.

Acknowledgements

This research was supported by the FONDECYT Projects 1961108 and 1990050, Universidad de Chile DID Project I001/99-2 and a CNRS/CONICYT 2000 Project UMR Géosciences Azur contribution no. 680. **[PD]**

References

Åberg, G., 1985. Open Rb–Sr systems due to burial metamorphism and some implications for dating. Geol. Fören. Stockh. Förh. 107, 127–132.

Åberg, G., Aguirre, L., Levi, B., Nyström, J.O., 1984. Spreading-subsidence and generation of ensialic marginal basins: an example from early Cretaceous of central Chile. In: Kokelaar, B.P., Howells, M.F. (Eds.), Volcanic and Associated Sedimentary and Tectonic Processes in Modern and Ancient Marginal Basins. Special Publication - Geological Society of London, vol. 16, pp. 185–193.

Aguirre, L., Levi, B., Nyström, J.O., 1989. The link between metamorphism, volcanism and geotectonic setting during the evolution of the Andes. In: Daly, J.S., Cliff, R.A., Yardley, B.W.D. (Eds.), Evolution of Metamorphic Belts. Special Publication - Geological Society of London, vol. 43, pp. 223–232.

Aguirre, L., Féraud, G., Morata, D., Vergara, M., Robinson, D., 1999. Time interval between volcanism and burial metamorphism and rate of basin subsidence in a Cretaceous Andean extensional setting. Tectonophysics 313, 433–447.

Coombs, D., 1960. Lower grade mineral facies in New Zealand. International Geological Congress Reports, 21 Session Norden, vol. 13, pp. 339–351.

Dong, G., Morrison, G.W., 1995. Adularia in epithermal veins, Queensland: morphology, structural state and origin. Miner. Depos. 30, 11–19.

Frey, M., De Capitani, D., Liou, J.G., 1991. A new petrogenetic grid for low-grade metabasitas. J. Metamorph. Geol. 9, 497–509.

Holland, T.J.B., Redfern, S.A.T., 1997. Unit cell refinement from powder diffraction data: the use of regression diagnostics. Mineral. Mag. 61, 65–77.

Kroll, H., Ribbe, P.H., 1987. Determining (Al, Si) distribution and strain in alkali feldspars using lattice parameters and diffraction-peak positions: a review. Am. Mineral. 72, 491–506.

Levi, B., Nyström, J.O., Thiele, R., Åberg, G., 1988. Geochemical trends in Mesozoic–Tertiary volcanic rocks from the Andes in central Chile and tectonic implications. J. South Am. Earth Sci. 1, 63–74.

McDougall, I., Harrison, T.M., 1999. Geochronology and thermochronology by the $^{40}Ar/^{39}Ar$ method. 2nd ed. Oxford University Press, NewYork. 269 pp.

Morata, D., Aguirre, L., Ruzziconi, Y., Féraud, G., Vergara, M., Puga, E., Díaz de Federico, A., 1997. Feldspar chemistry and preliminary Ar/Ar data on the lower Cretaceous basic lavas from the Coastal Range of Central Chile: petrogenetic implications. 8° Congreso Geológico Chileno, Antofagasta, T-II. , pp. 1385–1388.

Parada, M.A., Féraud, G., Fuentes, F., Aguirre, L., Morata, D., Paula Larrondo, P., 2004. Ages and cooling history of the Early Cretaceous Caleu pluton: testimony of a switch from a rifted to a compressional continental margin in central Chile. Geol. Soc. (in press).

Renne, P.R., Swisher, C.C., Deino, A.L., Karner, D.B., Owens, T., de Paolo, D.J., 1998. Intercalibration of standards, absolute ages and uncertainties in $^{40}Ar/^{39}Ar$ dating. Chem. Geol., Isot. Geosci. Sect. 145, 117–152.

Rivano, S., Sepúlveda, P., Boric, R., Espiñeira, D., 1993. Hojas Quillota y Portillo, V Región. Servicio Nacional de Geología y Minería, Carta Geológica de Chile No. 73 (escala 1: 250.000). Santiago.

Robinson, D., 1987. Transition from diagenesis to metamorphism in extensional and collision settings. Geology 15, 866–869.

Steiger, R.H., Jäger, E., 1977. Subcommission on geochronology: convention on the use of decay constants in geo-and cosmology. Earth Planet. Sci. Lett. 36, 359–362.

Stewart, D.B., Wright, T.L., 1974. Al/Si order and symmetry of natural alkali feldspars, and the relationship of strained cell parameters to bulk composition. Bull. Soc. Fr. Minéral. Cristallogr. 97, 356–377.

Vergara, M., Levi, B., Nyström, J., Cancino, A., 1995. Jurassic and early Cretaceous island arc volcanism, extension, and sub-

sidence in the Coast Range of central Chile. Geol. Soc. Amer. Bull. 107, 1427–1440.

Wall., R., Sellés, D., Gana, P., 1999. Area Tiltil-Santiago, Región Metropolitana. Servicio Nacional de Geología y Minería (Chile), Mapas Geológicos, No. 11 1 mapa escala 1: 100.000, 1 anexo. Santiago.

Wilson, N.S.F., Zentilli, M., Reynolds, P.H., Boric, R., 2003. Age of mineralization by basinal fluids at the El Soldado manto-type copper deposit, Chile: $^{40}Ar/^{39}Ar$ geochronology of K-feldspar. Chem. Geol. 197, 161–176.

York, D., 1969. Least squares fitting of a straight line with correlated errors. Earth Planet. Sci. Lett. 5, 324.